Rapid integrated biosensor for multiplexed immunoassays based on actuated magnetic nanoparticles†

D. M. Bruls, T. H. Evers, J. A. H. Kahlman, P. J. W. van Lankvelt, M. Ovsyanko, E. G. M. Pelssers, J. J. H. B. Schleipen, F. K. de Theije, C. A. Verschuren, T. van der Wijk, J. B. A. van Zon, W. U. Dittmer, A. H. J. Immink, J. H. Nieuwenhuis and M. W. J. Prins*

Received 13th July 2009, Accepted 8th September 2009
First published as an Advance Article on the web 15th October 2009
DOI: 10.1039/b913960e

The realization of biomolecular detection assays for diagnostic purposes is technologically very challenging because such tests demand full integration for ease of use and need to deliver a high analytical performance with cost-effective use of materials. In this article an optomagnetic immunoassay technology is described based on nanoparticles that are magnetically actuated and optically detected in a stationary sample fluid. The dynamic control of nanoparticles by magnetic fields impacts the key immunoassay process steps, giving unprecedented speed, assay control and seamless integration of the total test. The optical detection yields sensitive and multiplexed assays in a low-cost disposable cartridge. We demonstrate that the optomagnetic technology enables high-sensitivity one-step assays in blood serum/plasma and whole saliva. Drugs of abuse are detected at sub-nanogram per millilitre levels in a total assay time of 1 min, and the cardiac marker troponin I is detected at sub-picomole per litre concentrations in a few minutes. The optomagnetic technology is fundamentally suited for high-performance integrated testing and is expected to open a new paradigm in biosensing.

Introduction

In vitro diagnostics is a key element of modern health care and is of increasing importance due to the need for more effective and efficient health care. Currently about two-third of diagnostic tests is performed in centralized laboratories, hosting a large variety of analytical instruments which are operated by professional technicians. The remaining one-third of all tests is presently performed outside centralized laboratories in point-of-care settings. Point-of-care testing is technologically very demanding as the tests should be integrated for high ease of use and should deliver a high analytical performance in an uncontrolled environment at an affordable price. A very successful example of point-of-care testing is the measurement of glucose levels by diabetic patients. A 1 μL pinprick blood sample is inserted into a low-cost disposable strip and signals are recorded with a handheld reader. The enzyme-based assay technology underlying the glucose sensor is well suited for analytes in the millimolar concentration range, but cannot be applied to analytes that are present in very low concentrations, *e.g.* picomolar. To cover the low-concentration range, immunoassays employ high-affinity antibodies to detect analyte molecules with high-sensitivity and specificity. For decades the field of point-of-care immuno-biosensing has been dominated by lateral-flow chromatographic strips,[1,2] which is based on a continuous transport of sample fluid through a porous medium by capillary forces. Many point-of-care applications have requirements that cannot be served by the lateral-flow technology. Two such examples are the roadside screening for drugs of abuse in saliva for traffic safety, which is demanding on speed of the test, small sample volume and analyte multiplexing, and the detection of cardiac markers in blood, which puts high demands on sensitivity, precision, speed, and analyte multiplexing. This drives an intensive search for novel technologies that can deliver high test performance in an integrated format at affordable costs.

Several novel immunoassay detection technologies are being investigated, for example involving nanoparticle labeling,[3–5] label-free electrical detection,[6] fluorescence detection,[7,8] and labeling by oligonucleotides followed by biochemical amplification.[9] Most approaches focus on detection sensitivity or multiplexing, and not on the integration potential of the technology. The assays involve for example a sample dilution step or a transfer of analytes to a buffer fluid,[3–9] (bio)chemical development steps,[3,9] or wash steps with a buffer liquid.[3–9] Such process steps require storage of fluids as well as mechanical fluid actuation, which strongly decreases the integration potential, while adding to the total assay time and reagent use. In fact, the complete integration into a low-cost disposable cartridge of assays that are based on multiple fluid manipulations is harder to achieve than was envisioned more than a decade ago.[10]

In this article we propose a novel optomagnetic immunoassay technology that does not require the manipulation or replacement of fluids. The technology is based on nanoparticles that are magnetically actuated and optically detected in a stationary sample fluid. The dynamic control of nanoparticles by magnetic fields impacts all key immunoassay process steps, yielding unprecedented speed, assay control and seamless integration of

Philips Corporate Technologies, High Tech Campus, 5656 AE Eindhoven, The Netherlands. E-mail: menno.prins@philips.com; Tel: +31 40 27 48497
† Electronic supplementary information (ESI) available: Materials and methods. See DOI: 10.1039/b913960e

the different assay process steps. The optical detection enables sensitive and multiplexed assays with real-time detection of the binding processes, in a low-cost disposable cartridge.

Magnetically actuated immunoassay

We have designed a biosensor in which the key immunoassay process steps are controlled and accelerated by magnetic forces generated by electromagnets placed above and below the cartridge (see Fig. 1). We use superparamagnetic particles that have large field-induced magnetic moments.[11] The force on a magnetic particle scales with its magnetic moment.[12] This means that large particles with large magnetic moments are favorable for magnetic forces; however, in a biological assay the particles should not be too large because that generates steric hindrance for the biomolecular binding between particle and surface. We have developed an actuation system for particles with a diameter of a few hundred nanometres. The electromagnets are independently powered in order to generate fields with a tunable magnitude and orientation inside the 1 μL assay chamber of the cartridge. The assay process steps are depicted in Fig. 1a, exemplified with a sandwich immunoassay. In the first stage, dried-in magnetic nanoparticles are redispersed and mixed into the sample fluid that enters the cartridge. The redispersion process of the antibody-coated nanoparticles occurs in just a few seconds from a thin film of reagents. Subsequently the nanoparticles capture analyte molecules from the sample fluid. This is a rapid and efficient process due to the large total surface area of the dispersed nanoparticles. In the second stage, the electromagnets are used to move the nanoparticles (and the attached analyte molecules) through the bulk fluid and concentrate them at the binding surface. The particles are actuated in the vicinity of the sensor surface in order to allow rapid and specific biological binding of the nanoparticles to the sensor surface. In the third stage, unbound and weakly bound particles are removed from the surface by the application of a magnetic field from the upper magnet. A key advantage of using magnetic fields is that these are not perturbed by the biological matrix, so well controlled forces can be applied to the nanoparticles. Fig. 1b and c show the cartridge that is composed of two plastic parts, one with fluidic and the other with optical structures. The two plastic parts are joined by biocompatible double-sided adhesive tape that has been laser-cut in order to define a reaction chamber with a volume of 1 μL. Dry reagents containing magnetic particles and dry buffer components are placed as a thin layer in a cavity above the detection surface. The one-step assay format that we have developed requires only sample fluid to be applied onto the cartridge, with no extra fluid addition or fluidic wash steps.

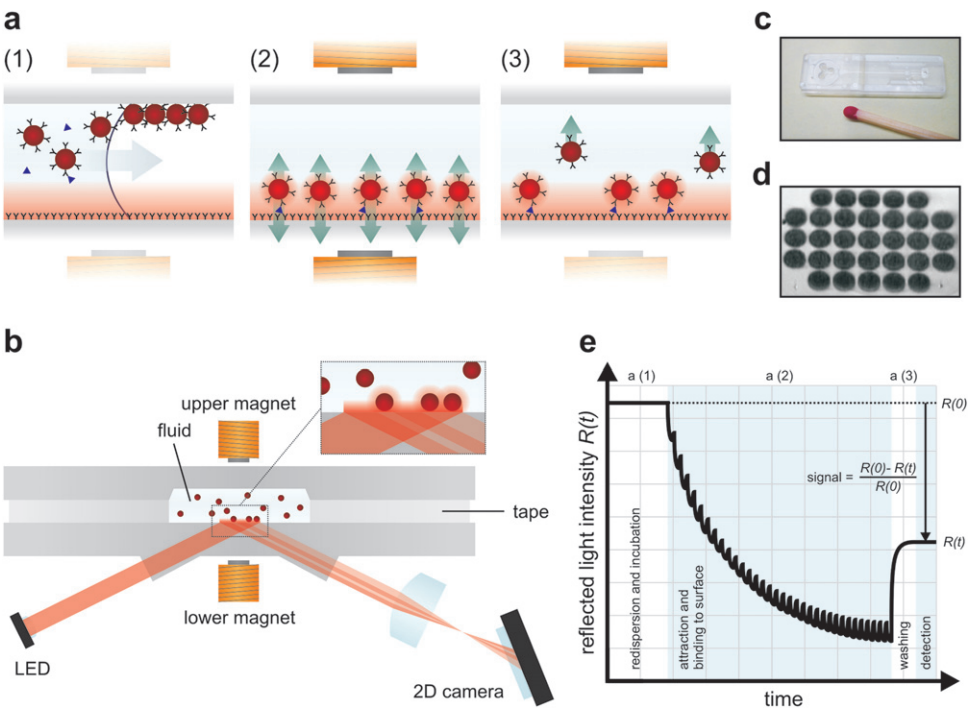

Fig. 1 Optomagnetic immuno-biosensor based on actuated magnetic nanoparticles. (a) Schematic representation of the reaction microchamber showing successively the assay processes: (a1) filling of the microchamber, nanoparticle redispersion, and capturing of analyte; (a2) actuation of the particles during the process of binding to the surface; and (a3) removal of free and weakly bound nanoparticles from the sensing surface by magnetic forces. (b) The fluid microchamber placed in the optomagnetic system with electromagnets and detection optics. Light reflects from the sensor surface with an intensity that depends on the concentration of nanoparticles at the sensor surface, by the mechanism of frustrated total internal reflection (f-TIR). (c) Picture of an assembled disposable cartridge consisting of two structured plastic parts connected by double-sided adhesive tape. The cartridge has outer dimensions of 1 cm × 4 cm. The cartridge contains a sample inlet, a channel, a reaction microchamber, and a vent. A total sample volume of 10 μL is supplied, of which 1 μL is analyzed in the reaction microchamber. (d) f-TIR image of magnetic nanoparticles bound to the sensor surface via an immunoassay on 31 capture spots of 125 μm diameter each. (e) Schematic real-time curve of the measured optical signal for a single capture spot. The assay phases a1–a3 are indicated. The signal modulation in phase a2 is caused by switched actuation of the magnetic nanoparticles.

Optical detection

Our biosensor requires a technology to sensitively monitor the presence of magnetic nanoparticles on the binding surface. The detection technique itself should be able to accommodate the placement of electromagnets close to the assay chamber, be insensitive to applied magnetic fields and should enable the parallel monitoring of many binding spots for assay multiplexing. We have applied the optical principle of frustrated total internal reflection (f-TIR)[13] for the detection of magnetic nanoparticles on the sensor surface, as sketched in Fig. 1b. A collimated beam of light from a light-emitting diode ($\lambda = 625$ nm) irradiates the sensor surface in a condition of total internal reflection, *i.e.* at an angle of incidence above the critical angle $\theta_{crit} = \arcsin(n_2/n_1)$, with n_1 and n_2 the refractive indices of the plastic cartridge and the medium in the cartridge, respectively (see ESI† for details). The condition of total internal reflection is met due to the fact that the refractive index of the cartridge plastic ($n = 1.53$) is higher than the refractive index of the medium inside the assay chamber (either air with $n = 1$, or an aqueous biological fluid with $n \approx 1.33$). A so-called evanescent optical field is generated at the plastic/fluid interface, which decays exponentially and penetrates into the fluid by only a sub-wavelength distance. In the starting situation without magnetic particles, no light is extracted from the evanescent optical field. The situation changes dramatically when magnetic nanoparticles are present at the sensor surface. The particles absorb and scatter part of the light, thus frustrating the total internal reflection and thereby reducing the intensity of the reflected light. An important advantage is the high signal per nanoparticle due to the detection of the total (*i.e.* 4π-steradians integrated) scattering and absorption, in contrast to detection principles that rely on light scattering into specific angles. The sensor surface is imaged onto a CCD camera. Fig. 1d shows an image of 31 capture spots of 125 μm diameter each, onto which magnetic nanoparticles have bound in an immunoassay. For a single binding spot, Fig. 1e sketches the light intensity of the reflected beam as a function of time for the different assay process steps. As indicated in Fig. 1e, the signal due to the presence of nanoparticles at the sensor surface is quantified by the reduction of reflected light intensity relative to the unperturbed total internal reflected light intensity prior to the binding of nanoparticles. The optical detection technique is highly suited in combination with magnetic actuation as the detection is insensitive to applied magnetic field and as the geometric conditions of f-TIR permit electromagnets to be situated directly above and below the assay chamber, where a high degree of assay control is needed.

We have characterized the sensitivity and speed of the optomagnetic system by recording signals of actuated magnetic nanoparticles in a model assay, namely an assay in which nanoparticles bind quickly and strongly to the detection surface (hit-and-stick assay). Fig. 2a shows the signal as a function of time for an assay with streptavidin-coated nanoparticles actuated toward an uncoated plastic surface. After injection of the fluid, the lower magnet was powered in order to generate a constant flux of particles toward the sensor surface. Fig. 2a shows a set of curves measured for different nanoparticle concentrations. The signals appear within the dynamic range of the present optoelectronic detection system, namely between the noise level of about 0.1% and nearly 100% for full surface coverage by magnetic particles. The curves show a linear signal increase in the first 10 s and signal saturation thereafter. The linear increase originates from the constant flux of nanoparticles toward the sensor surface, with an average particle velocity of about 20 μm s^{-1}. Saturation is reached when all nanoparticles in the fluid are bound to the surface and the fluid has become depleted of nanoparticles. The saturation signals can be used to derive a nanoparticle calibration curve of the detection system, indicated in Fig. 2b. The signal is proportional to the nanoparticle concentration across a wide concentration range. The linearity of the curve is a result of the linear dependency of the f-TIR signal on the particle concentration at the surface. The signal equals about 2% for a surface density of 1 nanoparticle per 10 μm^2, as was verified by counting nanoparticles on the sensor surface using an optical microscope.

Biological assays

The optomagnetic biosensor technology based on actuated nanoparticles can be used for the detection of a broad range of

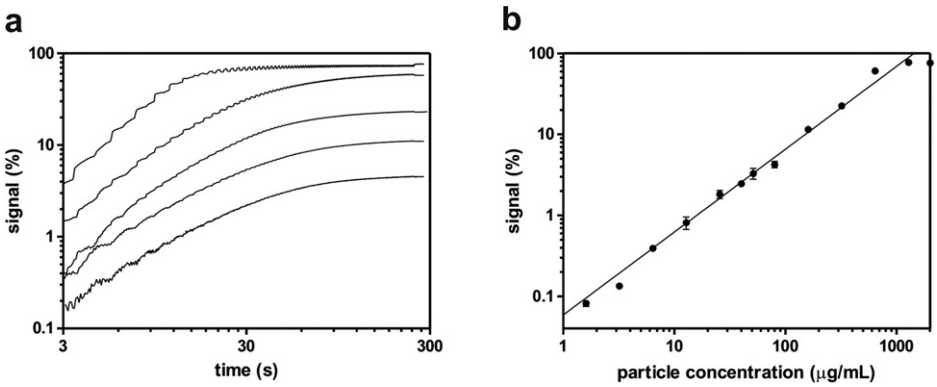

Fig. 2 Characterization of the sensitivity and speed of the optomagnetic system. (a) Real-time curves of the optical signal for streptavidin-coated magnetic particles with a diameter of 500 nm, attracted to an untreated sensor surface, for nanoparticle concentrations of 80, 160, 320, 640, and 2000 μg mL^{-1} (curves from bottom to top) in PBS. The magnetic field was applied with a strength of 3×10^4 A m^{-1}. (b) Calibration curve of the optical signal as a function of magnetic particle concentration. The curve is derived from the saturation values of curves as in part (a). The linear fit shows that the optical signal is proportional to the nanoparticle concentration over several decades.

biological molecules in affinity-based assays. To demonstrate the performance of the biosensor, we have developed a variety of competition/inhibition and sandwich immunoassays that have strong requirements on integration, speed and sensitivity. The roadside screening of motorists for the use of drugs of abuse (DoA) requires tests that (i) are integrated for easy use, (ii) run on an accessible sample type such as saliva, and (iii) can be performed with high speed in order not to disrupt traffic flow. One class of the drugs to be tested for is opiates. Opiates, such as morphine, are haptens that can be detected in a competition assay.[2] Highly specific antibodies are available that have been engineered to recognize opiates conjugated to bovine serum albumin (BSA) as well as the native drug molecules. In the rapid one-step assay that we have developed, a pure saliva sample enters an assay microchamber with magnetic nanoparticles and an optical detection surface. The nanoparticles are functionalized with anti-morphine antibodies and dried into a cavity in the assay microchamber (see ESI† for preparation details). The optical detection surface is provided with morphine conjugated to BSA. Morphine molecules in the sample bind to the antibodies on the magnetic particles and inhibit their binding to the sensor surface. Fig. 3a displays the real-time behavior of magnetic particles in an ultrafast morphine inhibition assay at two drug concentrations, 0 and 48 ng mL^{-1}, under magnetic actuation and optical detection. In the first 32 s the magnetic particles redisperse in the sample and bind morphine. Thereafter they are pulled toward the detection surface by the application of a magnetic field from the lower magnet. In the binding phase between 32 and 58 s, the particles are subjected to actuation from the lower magnet that is alternatively switched on and off. The particles are pulled toward the surface when the field is on, and the particles randomize their positions and orientations when the field is off. The switching of the magnetic field results in a modulation of the optical signal due to the dynamics of magnetic nanoparticles. The signal modulation is largest in the non-binding assay (48 ng mL^{-1}) because nanoparticles do not stick to the surface and have freedom of motion (the low-frequency undulation in the signal is a result of the fact that the optical sampling rate was of the same order of magnitude as the magnetic switching rate). In a final step at 58 s, unbound and weakly bound particles are removed from the surface by powering the upper magnet. Efficient control of the assay allows the morphine test to be performed, from the addition of raw sample to the final result, in a time of approximately 1 min. The morphine inhibition assay is quantitative and precise. Fig. 3b shows the average signal change as a function of morphine concentration ranging from 0.1 to 100 ng mL^{-1} in pure saliva, measured in a one-step assay with dry reagents inside the microchamber.

It is desirable to incorporate the simultaneous determination of several drugs of abuse into one single test, including morphine, amphetamine, methamphetamine, tetrahydrocannabinol, and cocaine. In the multiplexed assay format, individual spots containing drug conjugate for each drug are printed onto the detection surface and the magnetic particles with the corresponding antibodies are applied in a dry form above the detection area in a cavity. We employ inkjet printing to deposit biomaterials on the detection surface because it allows rapid production of functionalized cartridges and precise localization of spots with different binding molecules, suitable for a high degree of analyte multiplexing. Fig. 3c displays an f-TIR image of a multiplex assay for morphine, amphetamine, methamphetamine, tetrahydrocannabinol, and cocaine at various drug concentrations. The

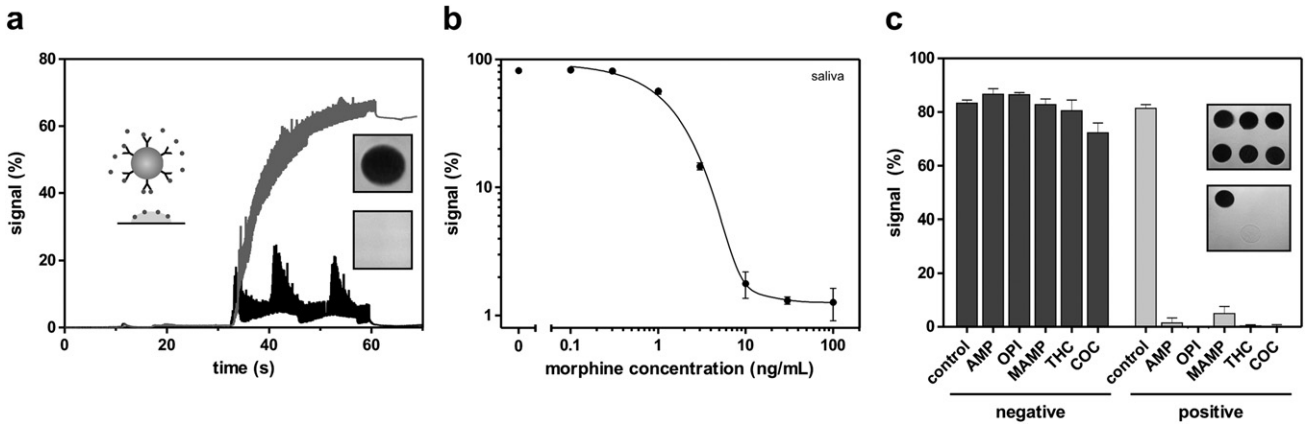

Fig. 3 Detection of drugs of abuse in saliva. (a) Real-time trace of the optical signal during a competitive immunoassay for morphine, for concentrations of 0 ng mL^{-1} (grey curve) and 48 ng mL^{-1} (black curve) in 100% saliva. In the first phase, dried nanoparticles redisperse and bind morphine molecules in the sample. In the second phase, nanoparticles are attracted to the sensor surface with the lower magnet. In the third phase, weakly bound and unbound particles are removed with a magnetic force directed away from the surface using the upper magnet. The inset shows the molecular architecture (morphine in solution, nanoparticles coated with anti-morphine antibodies, BSA–morphine on the sensor surface). Optical f-TIR images are shown of the spots after magnetic particle removal, for 0 and 48 ng mL^{-1} morphine. (b) Calibration curve of the optical signal as a function of morphine concentration in 100% saliva, determined after the magnetic removal step, for a magnetic nanoparticle assay with dry reagents inside the microchamber. For comparison: the cut-off level for morphine in saliva is 30 ng mL^{-1} in the preliminary guidelines of the SAMHSA (Substance Abuse Mental Health Services Administration) drug advisory board. The line is a guide to the eye. (c) Multiplexed competitive immunoassays in 100% saliva, for the five drugs amphetamine (AMP), morphine (OPI), methamphetamine (MAMP), tetrahydrocannabinol (THC), and cocaine (COC), and a control (anti-biotin coated nanoparticles bind to biotinylated-BSA on the sensor surface). Results of a negative multiplexed assay (all five drugs at 0 ng mL^{-1}) and results of a positive multiplexed assay (AMP: 80 ng mL^{-1}, OPI: 48 ng mL^{-1}, MAMP: 80 ng mL^{-1}, THC: 800 ng mL^{-1} and COC: 48 ng mL^{-1}) are shown. Data represent averages and standard deviations of 5 repetitions on different cartridges.

sixth spot consists of a control biotin assay. Using the current optics and electromagnets more than 30 spots of 125 μm diameter can be simultaneously imaged (see Fig. 1d). The number of spots imaged, and thus the number of detectable analytes, can be extended to several hundreds by using optics with a larger field of view and corresponding electromagnets. For the detection of multiple analytes which can cross-react, it is possible to physically separate the spots and nanoparticles of cross-reacting species in different microchambers in the cartridge.

The competition assay results as described above demonstrate that the biosensor can be used for precise ultrafast assays. For high-sensitivity determinations it is preferable to use the sandwich immunoassay format. We have developed a fully integrated rapid test for the detection of the protein cardiac troponin I (cTnI). Cardiac troponin I is a gold standard for the diagnosis of acute myocardial infarction (AMI).[14] The determination of cTnI has strict requirements in precision and high requirements for sensitivity as patient blood levels of cTnI at several picomolar or above have important clinical consequences.[15] Because of the urgent nature of AMI, it is desirable to have a test that is able to deliver lab-quality results in a rapid and integrated format, which can be used by non-technical care providers at point-of-care settings. We have developed a fast and sensitive cTnI test based on actuated magnetic nanoparticles. Fig. 4a displays the time evolution of the sensor signal for cTnI at 0 and 1000 pM (see ESI† for assay details). Nanoparticles were incubated for 30 s with the sample outside the cartridge and then injected into the cartridge. After the assay solution was introduced into the cartridge, the actuation protocol was initiated and particles carrying cTnI were collected at the surface using magnetic forces from the lower magnet, resulting in an increase of optical signal. The collection process has contributions perpendicular to as well as parallel to the surface (the increase of slope at approximately 80 s coincides with the arrival of laterally collected particles, as was verified using optical microscopy). Once reaching the surface, particles containing cTnI bind to the anti-cTnI functionalized detection surface. In the binding reaction a gentle actuation scheme is employed, tailored to the reaction between cTnI and the antibody. Since in low-concentration assays every magnetic particle contains on average less than one cTnI molecule, it is advantageous to expose all sides of the particles to the sensor surface. Furthermore, there will be a substantial amount of magnetic particles that cannot bind to the sensor due to the absence of analyte on their surface. We have found that the application of switched magnetic fields is most favorable for biological binding, since it generates a continuous rotational and translational rearrangement of the particles and thereby optimizes exposure of particles to the sensor surface. The magnetic fields are alternatively switched between a parallel and perpendicular orientation to the sensor surface, with short intermittent periods without magnetic field for diffusive relaxation of particles, as is illustrated in Fig. 4b. As magnetic particles tend to arrange in line with the magnetic field, the process results in alternating in-plane and out-of-plane particle arrangements relative to the sensor surface. The three-stage actuation strategy is designed (i) to efficiently bring particles from the bulk to the sensor surface, (ii) to randomize the particles for optimal exposure to the sensor surface, and (iii) to minimize non-specific binding by keeping the particles in constant motion relative to the sensor surface. The binding reaction proceeds under switched actuation for 4 min. It can be clearly observed in Fig. 4a that the rate at which the f-TIR signal increases is greater for an assay in which more particles bind. Particles that bind to the sensor surface give a higher contribution to the signal as they are on average closer to the surface than unbound particles. As a consequence it is possible to perform analyte quantifications

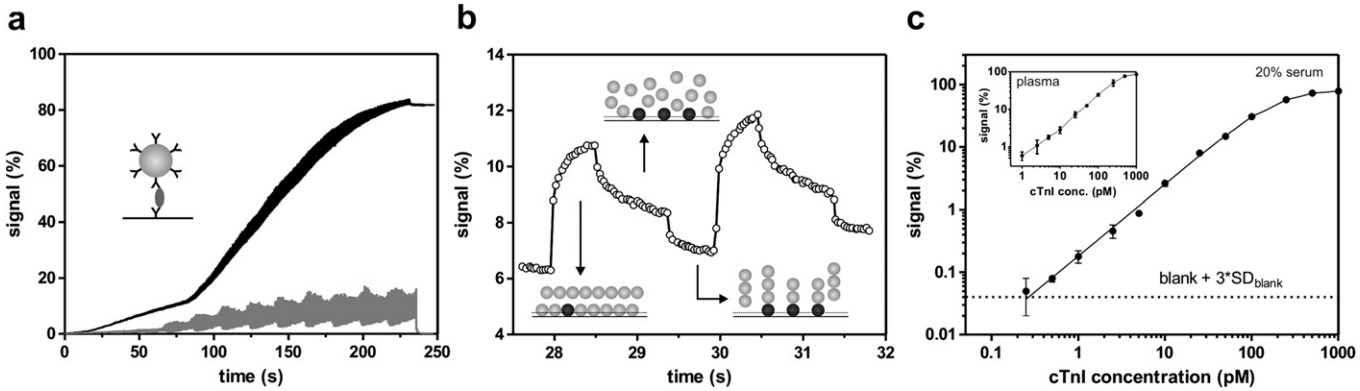

Fig. 4 Detection of troponin I in serum and plasma. (a) Real-time trace of the optical signal during a sandwich assay for cTnI, for concentrations of 0 pM (grey curve) and 1000 pM (black curve) in 20% human serum in PBS. Nanoparticles were mixed with the sample outside the cartridge. After injection into the cartridge, a switched actuation protocol was started and nanoparticles bind to the sensor surface. After 225 s, weakly bound and unbound particles were removed with a magnetic force directed away from the sensor surface using the upper magnet. The inset shows the molecular sandwich architecture, *i.e.* cTnI bound between antibody-coated nanoparticle and antibody-coated sensor surface. (b) A real-time curve of the optical signal from magnetic nanoparticles for a cTnI assay, displaying two cycles of the switched magnetic actuation sequence that is applied to bind magnetic particles to the sensor surface. In the first section, the signal increases as particles form arrangements parallel to the sensor surface. In the second section, the magnetic fields are turned off and particles have full translational and rotational freedom. In the third section, magnetic fields are applied to form particle arrangements perpendicular to the surface. (c) Calibration curve of the optical signal as a function of cTnI concentration in 20% human serum. Nanoparticles were mixed with the sample prior to injection into the cartridge. Signals were determined after the magnetic removal step. The inset shows a calibration curve of the integrated magnetic nanoparticle assay for cTnI in 100% plasma, with dry reagents inside the microchamber. Lines are guides to the eye. Data represent averages and standard deviations of 3 repetitions on different cartridges.

based on a kinetic fit of the real-time curve at very short assay times. A final magnetic separation step further improves the signal-to-blank ratio, the limit of detection and the precision by removing unbound and non-specifically bound particles.

High-sensitivity sub-picomolar detection of cTnI can be achieved with the optomagnetic technology in a total assay time of 5 min. Fig. 4c displays the calibration curve for a cTnI assay in human serum in which the particles are allowed to react with the protein for 30 s before injection into the cartridge, followed by an actuation protocol in the cartridge as described above. The obtained limit of detection, determined by three-fold the standard deviation of the blank signal, is 250 fM. The accurate control of all assay reactions including the bound/free separation results in a high precision. Coefficients of variations of less than 10%, with the majority of points having variations less than 5%, are achieved for signal changes greater than 0.5%. The measuring range before signal saturation is about three orders of magnitude (0.5–500 pM) and a signal-to-blank ratio of 2300 is achieved for 500 pM. A power fit in the range between 0.25 and 250 pM indicates that the curve is slightly superlinear with a power of 1.19 ($R^2 > 0.99$). A near-linear relationship between signal and concentration is highly desirable for precise analyte quantification. Strongly sub-linear dose–response curves have been reported for magnetic nanoparticle immunoassays without magnetic actuation;[5] the sub-linear behavior translates small signal errors into large uncertainties in the concentration determination of an unknown sample.

We have also developed a one-step cTnI assay with dry magnetic particles in the microchamber, for use with 100% plasma samples. In this assay, the protocol starts with a 90 s period of no applied field, in which the particles coated with anti-cTnI antibodies redisperse from the dry reagent into the plasma sample in the microchamber and react with the cTnI in solution. A calibration curve for cTnI in 100% human plasma using dry magnetic particles in the microchamber is shown in the inset of Fig. 4c. The limit of detection for this assay was found to be 3 pM. The higher limit of detection is due to higher non-specific interactions encountered in pure plasma. Further optimization of the buffer components for dry particles is required in order for the cTnI assay in pure plasma to achieve a detection limit similar to the assay in 20% human serum.

Discussion and outlook

The key demonstration of the present article is that sophisticated actuation of magnetic nanoparticle labels allows the full integration of immunoassays with high analytical performance. We have demonstrated that the technology enables high-sensitivity, one-step, dry-reagent assays in very small samples of blood plasma and whole saliva, with a total assay time of a few minutes. The short assay time originates from (i) efficient capture of analyte molecules by antibody-coated nanoparticles, (ii) rapid transport of nanoparticle–analyte complex to the sensor surface by magnetic forces, (iii) efficient binding to the sensor surface by switched actuation, and (iv) the rapid magnetic wash. The magnitude, orientation, and time-dependency of magnetic fields are electronically controlled, giving unprecedented control over the forces on and speeds of magnetic particles during the assay. The actuation principle opens a new paradigm in which multi-step assays can be performed in a stationary sample fluid, without requiring fluid transport or fluid replacement.

Magnetic nanoparticles were proposed as labels for affinity assays in 1978 by Ebersole.[16] Decades later, investigations started on detection using different types of sensors, for example magnetic coils,[17] SQUID,[18] microscopic imaging,[19] magneto-resistive sensors,[5,20,21] and Hall sensors.[22] In our magnetically actuated assays, detection is enabled by a novel optical scheme based on frustrated total internal reflection. The optical f-TIR method is intrinsically insensitive to magnetic fields, but very sensitive to magnetic nanoparticles. The technique allows the placement of electromagnets directly above and below the sensing surface where the most precise control of the assay is required. Another important advantage is that standard biocompatible plastic materials are used for the sensor cartridges, which are produced cost-effectively in large numbers by injection moulding. The functionalization of the plastic surfaces with various binding molecules is accomplished by using simple, well established, and characterized passive adsorption techniques. For covalent coupling of other molecules such as nucleic acids, surface treated plastic substrates are also widely available. The optomagnetic biosensor technology forms the basis for a range of further investigations, *e.g.* directed to assays with novel capture molecules and biological analytes, and assays with novel magnetic actuation schemes.

In summary, the presented optomagnetic biosensor technology based on actuated nanoparticles makes possible integrated, high-sensitivity, rapid, multiplexed assays on a small sample volume, in a low-cost disposable cartridge. We believe that the technology is fundamentally suited for point-of-care diagnostics and will open a new paradigm in biosensing.

Acknowledgements

The authors thank many colleagues in Philips Research, Philips Healthcare Incubator, Philips Applied Technologies, Concateno and Future Diagnostics for support and discussions. The work was partially funded by the NanoNed program of the Dutch Ministry of Economic Affairs.

References

1 P. Yager, T. Edwards, E. Fu, K. Helton, K. Nelson, M. R. Tam and B. H. Weigl, *Nature*, 2006, **442**, 412–418.
2 D. Wild, *The Immunoassay Handbook*, Elsevier, Amsterdam, 2005.
3 J. M. Nam, C. S. Thaxton and C. A. Mirkin, *Science*, 2003, **301**, 1884–1886.
4 Z. Chen, S. M. Tabakman, A. P. Goodwin, M. G. Kattah, D. Daranciang, X. Wang, G. Zhang, X. Li, Z. Liu, P. J. Utz, K. Jiang, S. Fan and H. Dai, *Nat. Biotechnol.*, 2008, **26**, 1285–1292.
5 S. J. Osterfeld, H. Yub, R. S. Gaster, S. Caramuta, L. Xu, S.-J. Han, D. A. Hall, R. J. Wilson, S. Sun, R. L. White, R. W. Davis, N. Pourmand and S. X. Wang, *Proc. Natl. Acad. Sci. U. S. A.*, 2008, **105**, 20637–20640.
6 G. Zheng, F. Patolsky, Y. Cui, W. U. Wang and C. M. Lieber, *Nat. Biotechnol.*, 2005, **23**, 1294–1301.
7 J. Todd, B. Freese, A. Lu, D. Held, J. Morey, R. Livingston and P. Goix, *Clin. Chem. (Washington, D. C.)*, 2007, **53**, 1990–1995.
8 R. Fan, O. Vermesh, A. Srivastava, B. K. H. Yen, L. Qin, H. Ahmad, G. A. Kwong, C.-C. Liu, J. Gould, L. Hood and J. R. Heath, *Nat. Biotechnol.*, 2008, **26**, 1373–1378.
9 S. Fredriksson, M. Gullberg, J. Jarvius, C. Olsson, K. Pietras, S. M. Gústafsdóttir, A. Östman and U. Landegren, *Nat. Biotechnol.*, 2002, **20**, 473–477.

10 A. van den Berg and T. S. J. Lammerink, in *Microsystem Technology in Chemistry and Life Sciences*, ed. A. Manz and H. Becker, Springer, Berlin, 1999, pp. 21–50.
11 A. H. Morrish, *The Physical Principles of Magnetism*, Robert E. Krieger Publishing Company, Inc., Huntington, New York, 1980.
12 A. Engel and R. Friedrichs, *Am. J. Phys.*, 2002, **70**, 428–432.
13 F. de Fornel, *Evanescent Waves: from Newtonian Optics to Atomic Optics*, Springer-Verlag, Berlin, 2001.
14 D. A. Morrow, C. P. Cannon, R. L. Jesse, L. K. Newby, J. Ravkilde, A. B. Storrow, A. H. B. Wu, R. H. Christenson, F. S. Apple, G. Francis and W. Tang, *Clin. Chem. (Washington, D. C.)*, 2007, **53**, 552–574.
15 M. C. Kontos, R. Shah, L. M. Fritz, F. P. Anderson, J. L. Tatum, J. P. Ornato and R. L. Jesse, *J. Am. Coll. Cardiol.*, 2004, **43**, 958–965.
16 R. C. Ebersole, *US Pat.*, 4 219 335, 1978.
17 C. B. Kriz, K. Rådevik and D. Kriz, *Anal. Chem.*, 1996, **68**, 1966–1970.
18 Y. R. Chemla, H. L. Grossman, Y. Poon, R. McDermott, R. Stevens, M. D. Alper and J. Clarke, *Proc. Natl. Acad. Sci. U. S. A.*, 2000, **97**, 14268–14272.
19 A. Perrin, A. Theretz, V. Lanet, S. Vialle and B. Mandrand, *J. Immunol. Methods*, 1999, **224**, 77–87.
20 D. R. Baselt, G. U. Lee, M. Natesan, S. W. Metzger, P. E. Sheehan and R. J. Colton, *Biosens. Bioelectron.*, 1998, **13**, 731–739.
21 W. U. Dittmer, P. de Kievit, M. W. J. Prins, J. L. M. Vissers, M. E. C. Mersch and M. F. W. C. Martens, *J. Immunol. Methods*, 2008, **338**, 40–46.
22 T. Aytur, J. Foley, M. Anwar, B. Boser, E. Harris and P. R. Beatty, *J. Immunol. Methods*, 2006, **314**, 21–29.

